Iontophoresis of Poly-L-lysines: The Role of Molecular Weight?

Norris G. Turner,[1,2] Laura Ferry,[3] Matthew Price,[1] Christopher Cullander,[1] and Richard H. Guy[1,4]

Received April 14, 1997; accepted July 7, 1997

Purpose. (1) To determine the extent of iontophoretic transport as a function of molecular weight (MW) of the penetrant; and (2) to visually and quantitatively characterize the iontophoretic transport pathways (follicular (F) versus nonfollicular (NF)) of the fluorescently-labeled poly-L-lysines employed.

Methods. A series of fluorescently-labeled poly-L-lysines (FITC-PLLs) [4 KDa, 7 KDa and 26 KDa] were used to study the extent and distribution of iontophoretic skin penetration as a function of MW using laser scanning confocal microscopy (LSCM).

Results. It was found that, relative to the passive controls, and under the electrical conditions considered, iontophoresis greatly enhanced the penetration of the 4 KDa analog, slightly elevated the delivery of the 7 KDa FITC-PLL, but had no effect on the transport of the larger 26 KDa FITC-PLL. Quantitative analyses of LSCM images revealed that iontophoresis increased transport via F pathways *only slightly* more than that through NF pathways for the 4 KDa and 7 KDa FITC-PLL molecules.

Conclusions. It is *visually* apparent that the iontophoretic transport pathways taken are importantly determined by the physicochemical properties (including size and charge) of the penetrant. The results presented here demonstrate an inverse dependence of iontophoretic delivery upon the MW of the penetrant.

KEY WORDS: iontophoresis; molecular weight; skin; confocal microscopy; drug delivery.

INTRODUCTION

The ultimate aim of this work is to expand the range of drugs for which transdermal drug delivery is a viable route of administration. Iontophoresis—the facilitation of (ionizable) drug delivery across the skin by an applied electrical potential—offers one approach by which this objective may be realized. In particular, the use of iontophoresis for the systemic delivery of new peptide and protein therapeutic agents from the biotechnology industry has attracted considerable recent interest (1). It follows, therefore, that the ability of iontophoresis to deliver drugs of relatively high molecular weight (MW), in a controlled and reliable fashion, is an issue of much importance

Although iontophoretic enhancement has been demonstrated for a number of "high" MW solutes including: angiotensin (2), luteinizing hormone releasing hormone (3), insulin (4), arginine-vasopressin (5), thyrotropin releasing hormone (6), and oligonucleotides (7), the *specific* effect of solute molecular size on the efficiency of iontophoretic transport has not been well-characterized, and a systematic investigation of the effect of MW on iontophoresis has yet to be undertaken. Of the few studies reported in the literature, Green *et al.* showed that, for a series of anionic penetrants (chloride ion, amino acids, N-acetylated amino acid derivatives, and tripeptides) ranging in MW from 35 to 443, the normalized flux varied inversely with MW. Similarly, Yoshida and Roberts (8), who investigated the iontophoretic transport of several (anionic, cationic and neutral) compounds, spanning MWs from 18 to 395, across human skin *in vitro*, demonstrated that solute molecular size was a major determinant of the efficiency of iontophoretic delivery. However, while this research contributes significantly to the mechanistic understanding of iontophoresis, the extent to which the results can be extrapolated to larger, or to more highly-charged, species is not known.

In the study presented here, we have initiated work to examine whether there exists a "cut-off" value of MW for iontophoretic delivery. A series of cationic poly-L-lysines of MWs 4 KDa, 7 KDa and 26 KDa were used because it has been suggested that such polypeptides can serve as valuable models for the study of diverse aspects of peptide and protein drug delivery (9,10). The transport into and within the skin of fluorescently-labeled poly-L-lysines (FITC-PLLs) has been monitored by laser scanning confocal microscopy (LSCM). Standard fluorometry has been employed to estimate the delivery of the same compounds across the skin. The specific aims of this investigation were, therefore, (1) to determine the extent of iontophoretic transport as a function of MW; and (2) to visually and quantitatively characterize the iontophoretic transport pathways (follicular (F) versus nonfollicular (NF)) of the fluorescently-labeled PLLs employed.

MATERIALS AND METHODS

Chemicals

FITC-PLLs of 4, 7 and 26 KDa [Peptide Technologies, Gaithersburg, Maryland] with average MWs of 3.7, 7.1 and 26 KDa, respectively, were employed in all transport experiments. The FITC labeling ranged from 0.0103 to 0.0760 mol FITC/mol lys. *N*-2-hydroxyethyl-piperazine-*N'*-2-ethanesulfonic acid (HEPES) and NaCl were obtained from Sigma Chemical Company (St. Louis, Missouri). Deionized water, of resistivity ≥ 18 MΩ cm^{-1}, from a Milli-Q UF Plus purification system (Millipore Corp., Bedford, MA), was used to prepare all aqueous solutions.

Electrodes

Ag/AgCl electrodes were used in all iontophoresis experiments. Details of their preparation were described previously (11).

[1] Departments of Biopharmaceutical Sciences and Pharmaceutical Chemistry, University of California—San Francisco, San Francisco, California 94143-0446.

[2] Current address: Department of Molecular Pharmacology, Stanford University School of Medicine, Stanford, California 94305-5332.

[3] Drug Delivery Systems, Novartis, East Hanover, New Jersey 07936.

[4] To whom correspondence should be addressed at Centre Interuniversitaire de Recherche et d'Enseignement, "Pharmapeptides", Campus Universitaire, Parc d'Affaires International, F-74166 Archamps, France. (e-mail: rhg@pharma1.cur-archamps.fr)

0724-8741/97/1000-1322$12.50/0

Experimental Apparatus

Iontophoresis experiments *in vitro* were performed in glass diffusion cells (Laboratory Glass Apparatus, Berkeley, California) (12). Constant current was supplied from a custom-built power supply (Professional Design and Development Services, Berkeley, California) interfaced to a MacIntosh IIfx computer (Apple Computer Inc., Cupertino, California) running LabView 2.1.1 software (National Instruments Inc., Austin, TX). A Bio-Rad MRC 600 Laser Scanning Confocal Microscope (LSCM) (Bio-Rad Microscience Ltd., Hemel Hempstead, UK) was employed for imaging.

Fluorometric measurements were performed using a Spex Fluorolog 1680 0.22 m Double Spectrometer (SPEX Industries, Inc., Edison, New Jersey). The excitation and emission wavelengths were 495 and 518 nm, respectively.

EXPERIMENTS

Iontophoresis

Eight to twelve-week old HR/hrs female hairless mice (Simonsen, Gilroy, CA), sacrificed by CO_2 euthanasia, provided skin for the transport experiments. The skin separated the donor and the receptor compartments of the diffusion cell. Electrolyte solution (25 mM HEPES buffer in 133 mM NaCl, adjusted to pH 7.4), degassed under vacuum prior to usage, was introduced into the "non-working" electrode chamber (i.e., cathode) and into the receptor compartment. The FITC-PLL solution (0.05 mM in the same electrolyte solution) was placed in the donor, anode chamber. The electrodes were then inserted and connected to the power supply. The receptor solution was well-stirred throughout the experiment. Constant current at 0.5 mA/cm^2 was passed for 4, 8 or 16 hrs. All transport experiments were performed in triplicate on skin taken from 3 different mice. For each measurement, a passive (control) experiment was performed under identical conditions except that no current was passed. Each mouse served as its own control. Immediately after iontophoresis, the skin was removed from the diffusion cell and thoroughly rinsed with milli-Q water to remove any residual fluorescent material from the skin surface. Skin samples were wrapped in aluminum foil to protect against photobleaching and then taken immediately to the confocal microscope for imaging.

Measurement of the Extent of Transport

The amount of FITC-PLL delivered across the skin during the transport experiments was determined by fluorometric analysis of the receptor solution. A calibration curve for this purpose, and the necessary background corrections, were performed in a manner completely identical to that previously described for the analysis of calcein (11). Under no circumstances was any passive transport observed for these highly-charged species. The Mann-Whitney Rank test was used to compare the results between different iontophoresis experiments and between different PLLs.

Confocal Microscopy—Visualization

Post-iontophoresis, a 5 mm diameter biopsy of skin was mounted, without fixation, in a sample holder and covered with a glass coverslip for confocal viewing. All images were acquired with a 40× oil immersion lens (except when noted otherwise); the same laser intensity, filterblock, lens, gain, black level and scan speed were used. The selected laser line for FITC-PLL excitation was 488 nm. Unless otherwise stated, confocal images were obtained as z-series (11).

Experimentally, z-series were collected from three randomly selected skin sites from three different mice. The microscope stage coordinates were randomly generated by a computer algorithm. Thus, nine z-series were collected for each of the 4, 8, and 16 hr transport experiments. For the purposes of clarity, however, only one representative passive and iontophoretic z-series for each time point is displayed in the results section. All z-series consisted of 11 optical sections collected over the range 0–50 μm in 5 μm increments.

Confocal Microscopy—Quantification

To determine the autofluorescence properties of HMS, skin samples were first visualized, with both standard and enhanced gain and aperture settings, in the absence of FITC-PLLs. Analysis of the confocal images involved specifically: (1) assessment of the extent of iontophoretic delivery of FITC-PLLs into the skin (compared to the passive control); and (2) visualization and quantification of transported fluorophores along follicular (F) and nonfollicular (NF) (e.g., intercellular, transcellular) transport pathways.

The analysis was performed on iontophoresis images only, as insufficient fluorescence within the passive skin controls was present for accurate measurement. The quantitative transport data from confocal images were expressed as: (1) the absolute transport number—the fraction of the total transported fluorescence along a designated transport route (i.e., either F or NF); (2) the normalized transport number—the fraction of the total transported fluorescence *per unit area* along a designated transport route (i.e., either F or NF).

The quantitative measure of fluorescence intensity, obtained from the COMOS program, is called *Total Pixel (TP)* which is the integrated sum of the pixel values within a user-defined area. Each pixel in the confocal image is assigned a grey scale intensity value which ranges from 0 (black) to 255 (peak white). In each iontophoretic confocal image, surface area and pixel intensity were determined for the following anatomic regions (Figure 1): hair shaft (h), pilosebaceous unit (pil), follicular (F), nonfollicular (NF), total image area (tot), and transport area (trnprt). The corresponding TP values for these anatomic regions were also recorded. The following assumptions were made: (1) The surface area of the measured anatomic regions (e.g., h, pil, F, etc.) remain constant with increasing skin depth (i.e., 0–50 μm); it was arbitrarily decided to use the image in the z-series from 20 μm below the skin surface. (2) FITC-PLL transport through the hair shaft (h) itself did not occur, meaning that TP values from the hairs were zero.

This quantitative method assessed the relative contribution of the F and NF transport pathways for the iontophoretic penetration of the three model fluorescent penetrants at each sampled skin depth. FITC-PLL transport along the F and NF pathways within single confocal images (at each designated skin depth) were compared. For each iontophoresed skin sample, the calculated absolute and normalized transport number data from three z-series were averaged, and then plotted as a function of skin

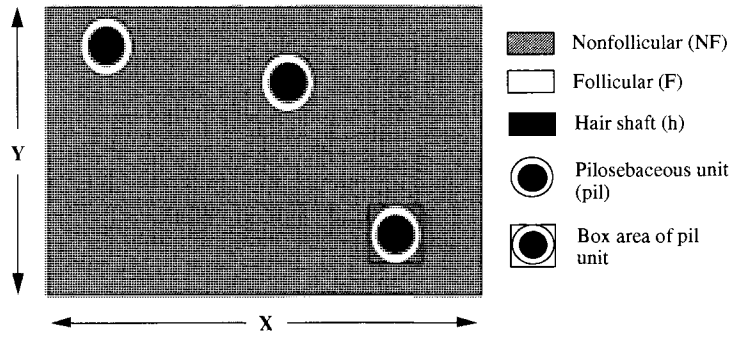

Surface Area Parameters

$A_{(h)}$ = Σ (areas occupied by hair shaft)

$A_{(pil)}$ = Σ (areas of pilosebaceous unit)

$A_{(F)}$ = area available for follicular transport = $A_{(pil)} - A_{(h)}$

$A_{(NF)}$ = area available for nonfollicular transport = $A_{(tot)} - A_{(pil)}$

$A_{(trnprt)}$ = area available for F and NF transport = $A_{(tot)} - A_{(h)}$

$A_{(tot)}$ = total surface area of confocal image = X * Y

Total Pixel Parameters

$TP_{(h)}$ = Σ (pixel intensity of hair shaft regions) = 0

$TP_{(pil)}$ = Σ (pixel intensity of pil units)

$TP_{(F)}$ = pixel intensity of F region = $TP_{(pil)} - TP_{(h)}$

$TP_{(NF)}$ = pixel intensity of NF region = $TP_{(tot)} - TP_{(pil)}$

$TP_{(trnprt)}$ = area available for F and NF transport = $A_{(tot)} - A_{(h)}$

$TP_{(tot)}$ = pixel intensity of whole confocal image = X * Y

Fig. 1. Schematic diagram of a LSCM image of HMS. Both surface area and pixel intensity parameters from F and NF regions of the image are acquired. All parameters were obtained using the Histogram feature in the COMOS Software Program. The area and intensity parameters from the different morphological regions of the imaged HMS (e.g., NF, F, h, pil) were then used to calculate the transport number values for F and NF pathways.

depth. Pathway transport numbers were determined for the F and NF pathways at sampled skin depths of 0, 15, 30, 40 and 50 μm below the surface within each z-series.

Statistical Analysis of Confocal Data

To evaluate the degree of inter-mouse variability in the pathway transport number data, a one-way analysis of variance compared the means and standard deviations of each of the three mice at each corresponding skin depth (0, 15, 30, 40 and 50 μm below the skin surface), followed, when significant differences were detected, by a Student-Newman-Keuls test.

Stability of Penetrant Molecules

To determine whether electrolytic or metabolic degradation of the FITC-PLLs was occurring, mass spectrometry was used to analyze the poly-lysine solutions, both before and after exposure to current and in the presence and absence of the skin.

RESULTS

Extent of Transport

The cumulative amounts of the FITC-PLLs delivered into the receptor solution following 4, 8 and 16 hr current passage are shown in Table I. Transport of the 4 KDa and 7 KDa FITC-PLLs increased with increasing duration of current passage. The extent of transport was significantly greater for the smaller species. No net transport of the largest species (26k) was observed.

Visualization of FITC-PLL Transport as a Function of MW

Typical z-series are shown in Figures 2–4. These images show the distribution of FITC-PLLs within the F and NF transport pathways of HMS *in vitro* as a function of MW. Enhanced

Table I. Cumulative Delivery of 4, 7 and 26 KDa FITC-PLLs Across HMS *in Vitro* Following 4, 8, and 16 hrs of Iontophoresis at 0.5 mA/cm²

Duration of transport (hrs)	Cumulative delivery of FITC-PLL (nmol)		
	4 KDa	7 KDa	26 KDa
4	n.m.	n.m.	n.d.
8	$0.96 \pm 0.37^{a,c}$	$0.11 \pm 0.03^{a,d}$	n.d.
16	$40.8 \pm 0.70^{b,c}$	$0.77 \pm 0.03^{b,d}$	n.m.

Note: Transport was measured fluorometrically as described in "Materials and Methods". n.m.—not measurable (signal below background). n.d.—not determined.

[a] Significantly different at $p < 0.05$.
[b] Significantly different at $p < 0.05$.
[c] Significantly different at $p < 0.05$.
[d] Significantly different at $p < 0.05$.

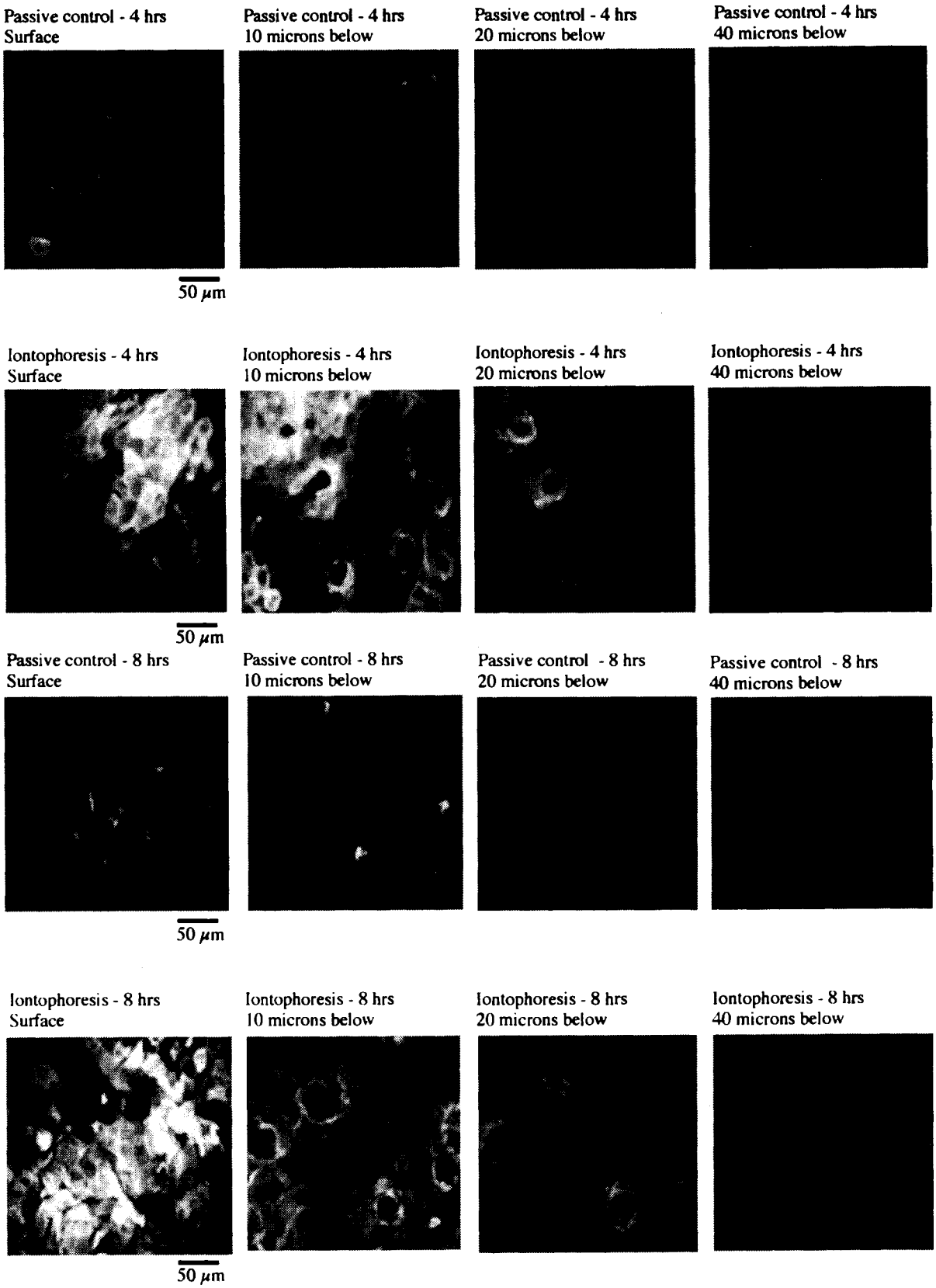

Fig. 2. (a) LSCM images of HMS after (i) 4 hrs passive diffusion of 4 KDa FITC-PLL (upper panel), and (ii) 4 hrs anodal iontophoresis of 4 KDa FITC-PLL (lower panel). In both series, the images correspond to optical sectioning at 0, 10, 20 and 40 μm below the skin surface (arranged from left to right). The magnification was 40× for all images. Scale bars are 50 μm. (b) LSCM images of HMS after (i) 8 hrs passive diffusion of 4 KDa FITC-PLL (upper panel), and (ii) 8 hrs anodal iontophoresis of 4 KDa FITC-PLL (lower panel). In both series, the images correspond to optical sectioning at 0, 10, 20 and 40 μm below the skin surface (arranged from left to right). The magnification was 40× for all images. Scale bars are 50 μm. (c) LSCM images of HMS after (i) 16 hrs passive diffusion of 4 KDa FITC-PLL (upper panel), and (ii) 16 hrs anodal iontophoresis of 4 KDa FITC-PLL (lower panel). In both series, the images correspond to optical sectioning at 0, 10, 20 and 40 μm below the skin surface (arranged from left to right). The magnification was 40× for all images. Scale bars are 50 μm.

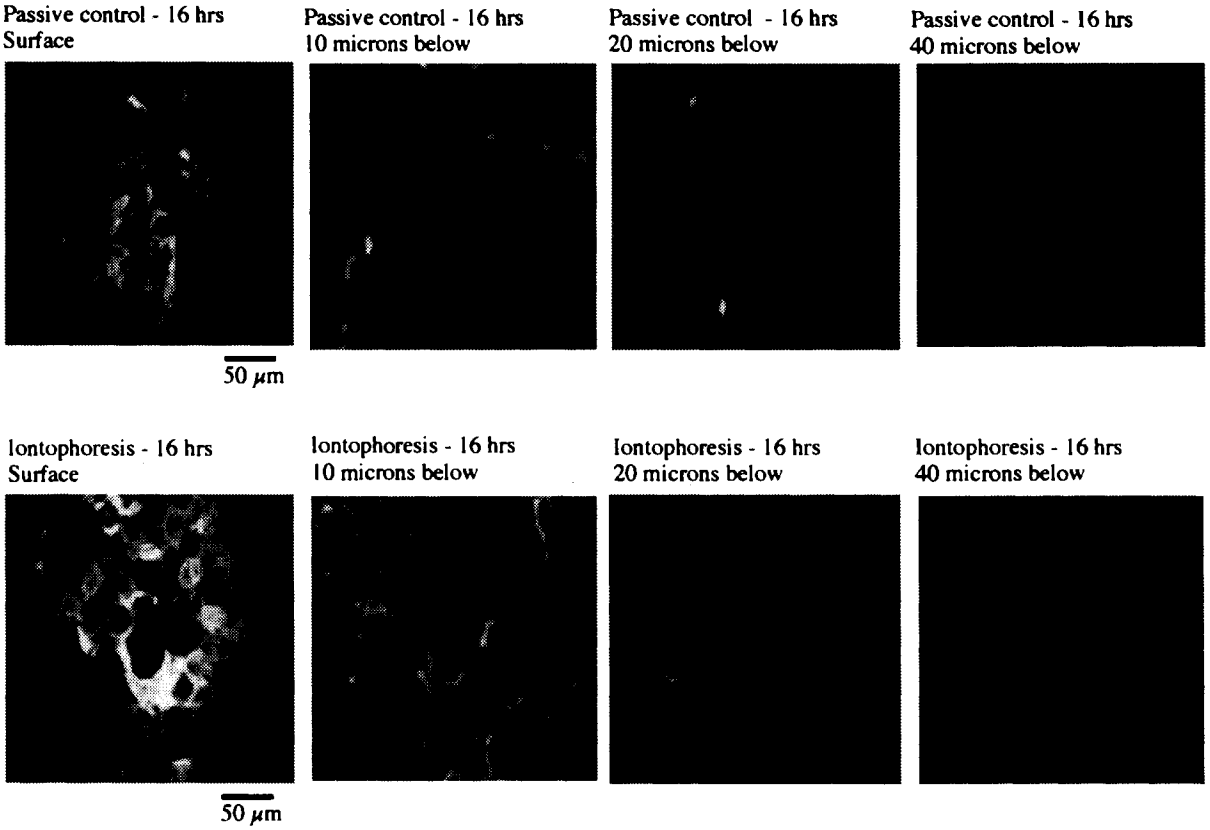

Fig. 2. Continued.

iontophoretic penetration of the 4 KDa species was clear (compared to the passive control) following 4, 8 and 16 hr transport (Figures 2a–c). Passive diffusion, on the other hand, was negligible. Iontophoresis of the 4 KDa FITC-PLL localized fluorescence primarily in the hair follicles, especially at the deeper levels of the skin (i.e., 20–40 μm below the surface). Iontophoretic penetration of the 4 KDa FITC-PLL into NF regions was considerable at levels ~10–15 μm below the surface, but then decreased apparently with increasing skin depth. For the 7 KDa FITC-PLL, iontophoretic enhancement was negligible for the 4 and 8 hr experiments (Figures 3a,b). Following 16 hr exposure to current, though, the apparent delivery of the 7 KDa FITC-PLL appeared moderately elevated relative to 16 hr of passive diffusion (Figure 3c). Once again, the enhanced penetration was noted primarily along the hair follicles. However, for the 26 KDa FITC-PLL, there was no enhancement over the passive control after 16 hr current passage (Figure 4). Consequently, transport experiments for 4 and 8 hrs were not conducted.

Quantification of FITC-PLL Transport

To complement the confocal visualization, quantitative analysis permitted objective assessment of the relative iontophoretic penetration of the FITC-PLLs along F and NF pathways. Evaluation was performed only on those images, in which significant iontophoretic enhancement (over the passive control) was observed. The plots of the *absolute* (and normalized) transport numbers of the FITC-PLLs as a function of skin depth (Figures 5a–c and 6) are the quantitative correlates of the images shown in Figures 2a–c and 3c (lower panels), respectively, for the 4 KDa and 7 KDa FITC-labeled PLLs. When uncorrected for surface area, iontophoretic transport of the 4 KDa and 7 KDa FITC-PLLs was significantly less via F pathways than through NF routes. However, when the fractional surface area occupied by the F structures (relative to NF regions of the skin) is taken into account (see the accompanying normalized pathway transport number versus skin depth graphs in Figures 5a–c and 6), much higher transport was observed via F pathways, especially within the deeper skin layers. For example, at 50 μm below the skin surface, 67% and 56% of the iontophoretic transport of the 4 KDa and 7 KDa species, respectively, occurred along the F route (relative to the NF pathway). To emphasize this point, it should be noted that, at 50 μm below the skin surface, F regions are estimated to account for only ~5–10% of the total surface area, a value not significantly different from the measured absolute transport numbers of the 4 KDa and 7 KDa FITC-labeled molecules. Thus, together with the corresponding LSCM images, it is evident from the absolute transport number data that current passage provoked enhanced transport by approximately equal amounts via F and NF pathways. Normalization with respect to relative surface area, however, reveals dramatically the important role for the appendageal structures.

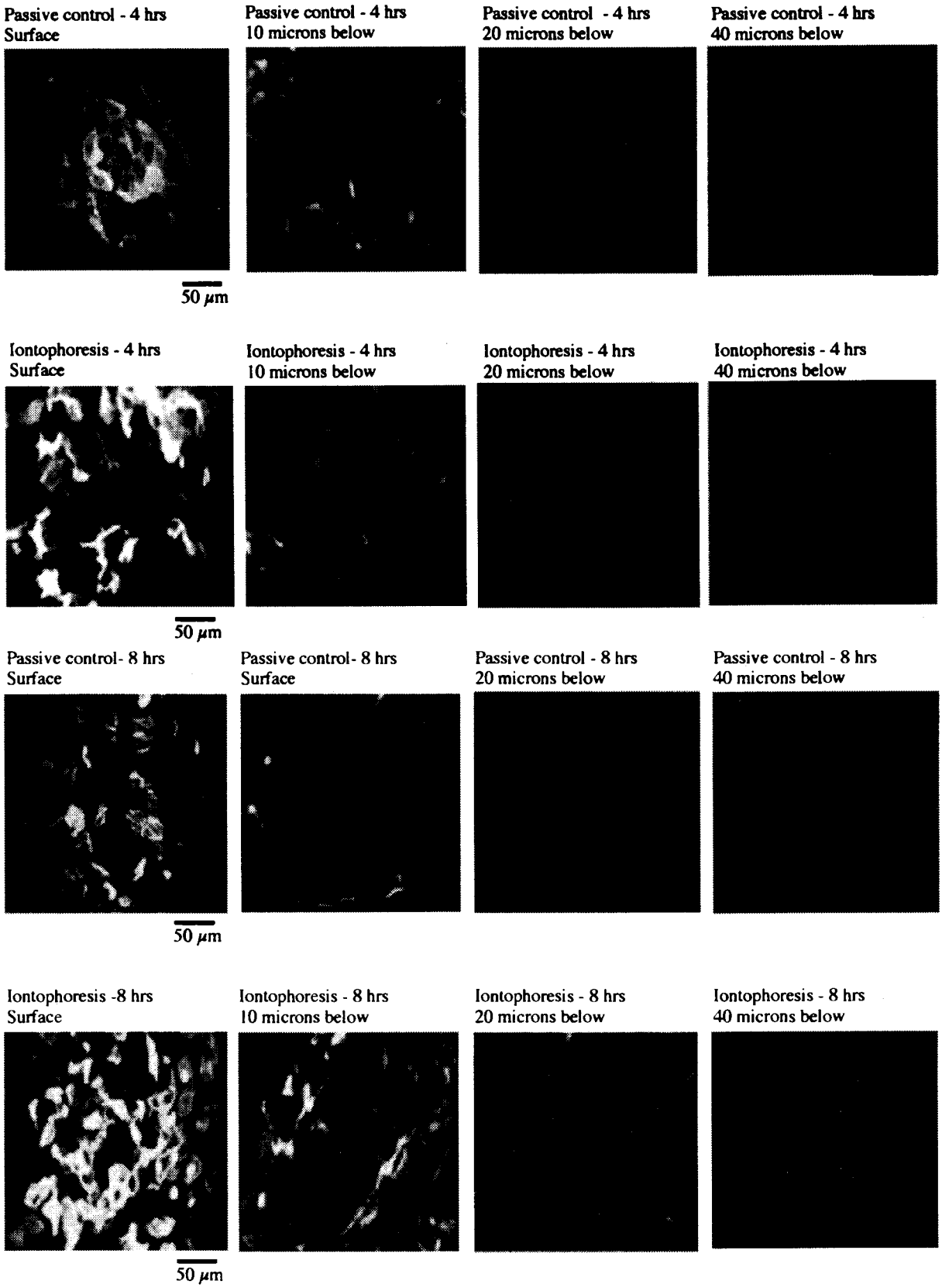

Fig. 3. (a) LSCM images of HMS after (i) 4 hrs passive diffusion of 7 KDa FITC-PLL (upper panel), and (ii) 4 hrs anodal iontophoresis of 7 KDa FITC-PLL (lower panel). In both series, the images correspond to optical sectioning at 0, 10, 20 and 40 μm below the skin surface (arranged from left to right). The magnification was 40× for all images. Scale bars are 50 μm. (b) LSCM images of HMS after (i) 8 hrs passive diffusion of 7 KDa FITC-PLL (upper panel), and (ii) 8 hrs anodal iontophoresis of 7 KDa FTIC-PLL (lower panel). In both series, the images correspond to optical sectioning at 0, 10, 20 and 40 μm below the skin surface (arranged from left to right). The magnification was 40× for all images. Scale bars are 50 μm. (c) LSCM images of HMS after (i) 16 hrs passive diffusion of 7 KDa FITC-PLL (upper panel), and (ii) 16 hrs anodal iontophoresis of 7 KDa FITC-PLL (lower panel). In both series, the images correspond to optical sectioning at 0, 10, 20 and 40 μm below the skin surface (arranged from left to right). The magnification was 40× for all images. Scale bars are 50 μm.

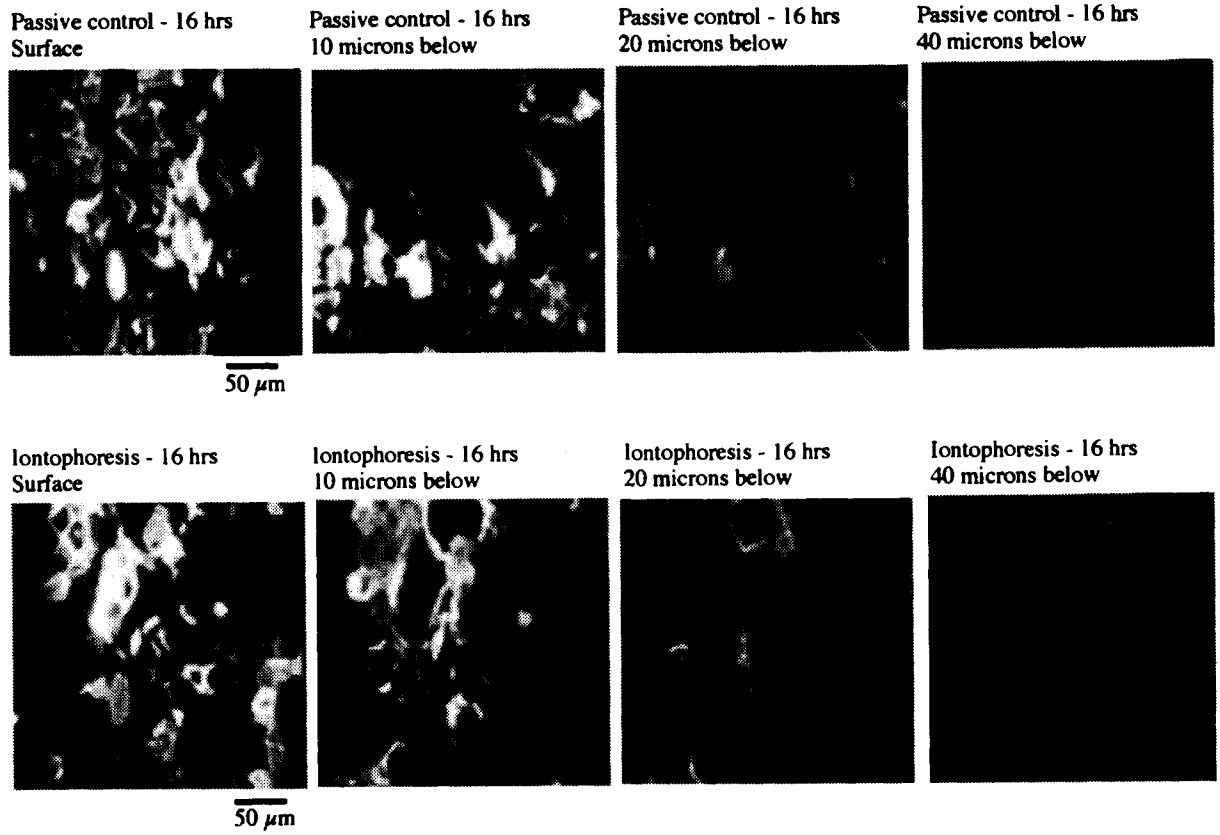

Fig. 3. Continued.

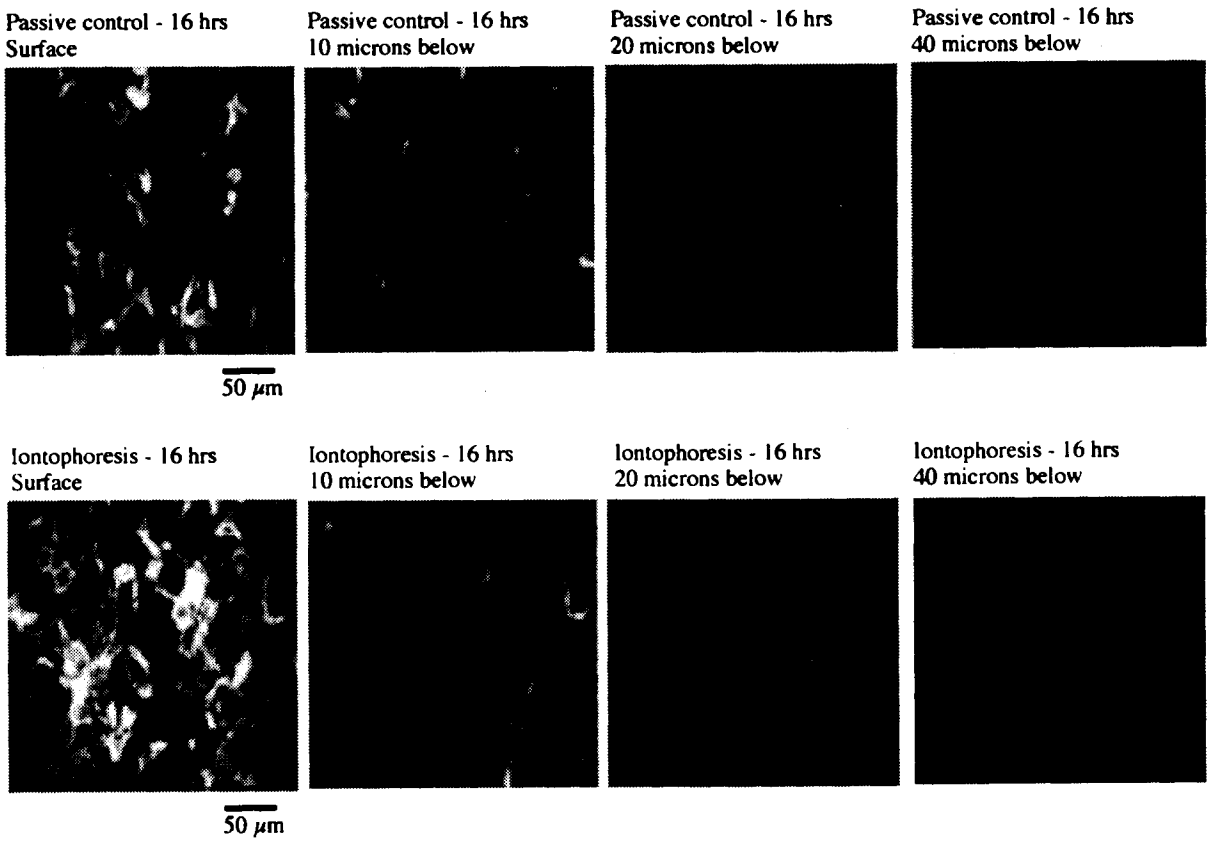

Fig. 4. LSCM images of HMS after (i) 16 hrs passive diffusion of 26 KDa FITC-PLL (upper panel), and (ii) 16 hrs anodal iontophoresis of 26 KDa FITC-PLL (lower panel). In both series, the images correspond to optical sectioning at 0, 10, 20 and 40 μm below the skin surface (arranged from left to right). The magnification was 40× for all images. Scale bars are 50 μm.

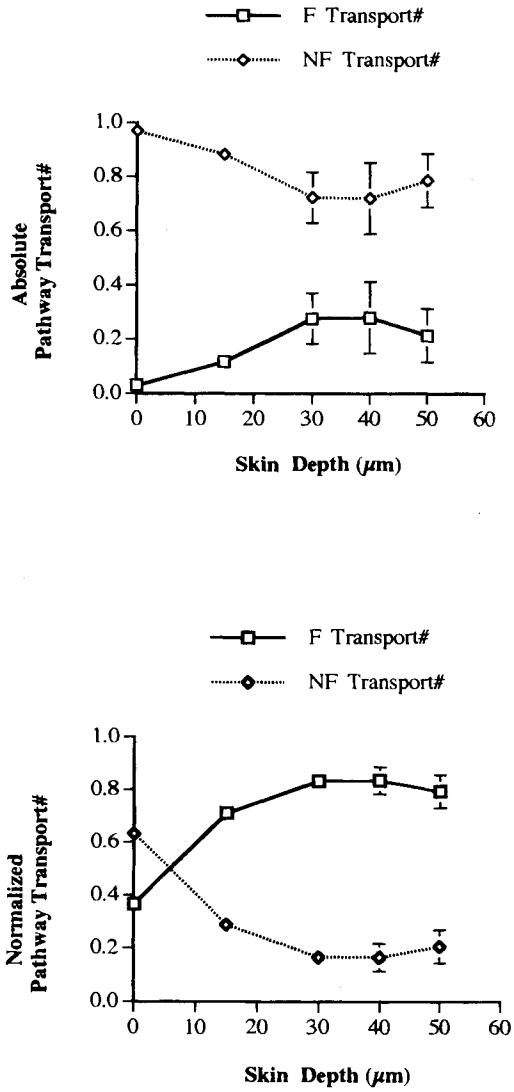

Fig. 5a. Anodal iontophoresis of 4 KDa FITC-PLL for 4 hrs: absolute (above) and normalized (below) transport number values, as a function of skin depth via F and NF routes in HMS. Averaged data from three different skin sites (mean ± SD) in a single mouse are presented.

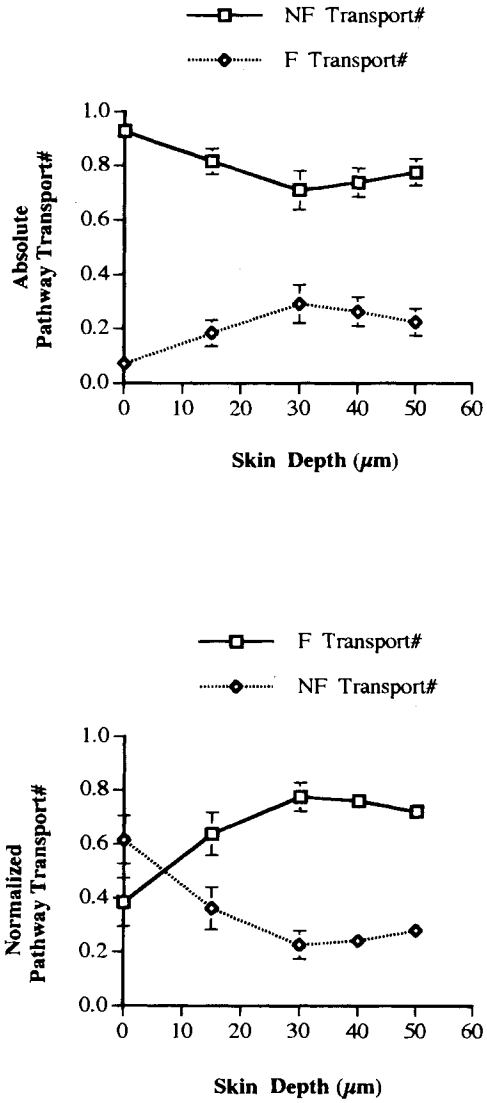

Fig. 5b. Anodal iontophoresis of 4 KDa FITC-PLL for 8 hrs: absolute (above) and normalized (below) transport number values, as a function of skin depth via F and NF routes in HMS. Averaged data from three different skin sites (mean ± SD) in a single mouse are presented.

Stability of the Penetrant Molecules

Following derivatization of the PLLs with FITC, size-exchange chromatography was used by the supplier (Peptide Technologies of Gaithersburg, Maryland) to purify the fluorescent probes, and low-angle laser light scattering was used to measure the average molecular weights (3.7 KDa, 7.1 KDa and 26 KDa). Mass spectrometry (conducted in the Protein and Carbohydrate Structure Facility at the University of Michigan) confirmed the average MWs of the three species (data not shown). After 16 hr exposure to current, the average MWs of the different peptides (removed either from the donor or the receptor solutions) were essentially unchanged, although their distribution was somewhat broader. Hence, it was concluded that the PLLs were largely resistant to degradation by either electrolysis or hydrolysis.

DISCUSSION

Passively, the penetration of the FITC-PLLs during 16 hrs was negligible. Under iontophoretic conditions, on the other hand, transport depended upon MW. Enhancement of the 4 KDa peptide was clear, and increased with increasing time of current passage. Delivery of the intermediate (7 KDa) PLL was much less efficient, while that of the largest fluorophore (26 KDa) was not detectable. While it would obviously be premature and unwarranted to deduce a MW "cut-off" from these results, it is apparent that, under the conditions of the experiment performed, for the class of molecule studied, little iontophoretic transport can be expected for compounds much greater than 10 KDa. It must be emphasized, however, that this conclusion should not be extrapolated to all peptide/protein delivery situations. Each case must, at least in part, be individually evaluated and will depend very significantly on the *potency* of the com-

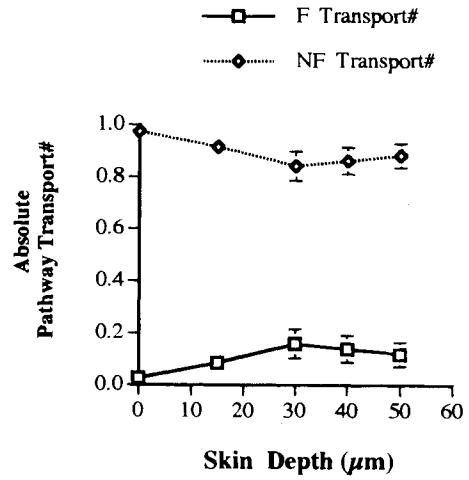

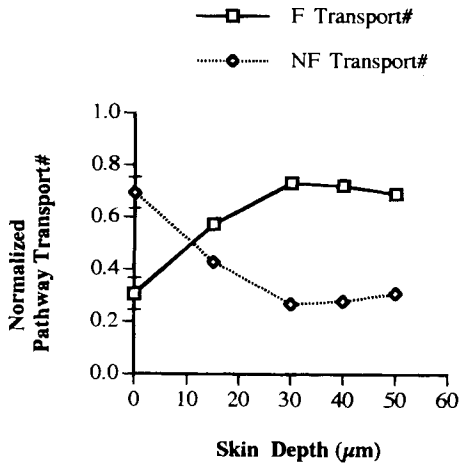

Fig. 5c. Anodal iontophoresis of 4 KDa FITC-PLL for 16 hrs: absolute (above) and normalized (below) transport number values, as a function of skin depth via F and NF routes in HMS. Averaged data from three different skin sites (mean ± SD) in a single mouse are presented.

pound to be delivered (i.e., the MW "cut-off" will clearly be higher for exquisitely potent molecules than for those of lesser potency). Other factors, including metabolic and electrochemical stability, may also play important roles.

The second key issue addressed here was the pathway of iontophoretic penetration. Appendageal routes have been implicated in the passive permeation of charged compounds across the skin (13), albeit at very low flux. With current, on the other hand, the appendages assume much greater significance (14–20). The importance of the sweat glands in iontophoresis across human skin is well-known (14,15,17). In HMS, which has no sweat glands, the follicles play a major role (18–21), which is confirmed here for the lowest MW PLL (Figures 2a–c). For the higher MW cations, however, iontophoretic delivery through the skin in general becomes less efficient (Figures 3a–c and 4).

In contrast to calcein (11), the PLLs were transported more significantly into the NF regions, especially deeper within the skin (20–40 μm). For example, after 16 hrs of iontophoresis of the 4 KDa PLL, the absolute NF and F transport numbers at 50 μm into the tissue reflected more-or-less exactly the relative surface areas of the two pathways; i.e., there was no preferential passage along a particular route.

Iontophoretic transport via a specific path will depend at least upon (a) the physicochemical properties of the penetrant, (b) the 'depth' within the skin (i.e., SC versus viable epidermis versus dermis), and (c) the conditions of the experiment (pH, electrolyte, buffer, current profile, etc.). The greater apparent affinity of PLLs for NF (i.e., intercellular lipid bilayers) regions of the skin (relative to calcein) may be related to their intrinsic attraction to epithelial membranes. In fact, polycations are known to affect epithelial permeability under certain circumstances (22). However, PLLs only minimally alter hydrocarbon chain packing in lipid bilayers (23) and cannot be expected, under the conditions of this study, to have any chemical penetration enhancing effects on the skin. This does not mean, though, that association of PLLs with the intercellular bilayers is impos-

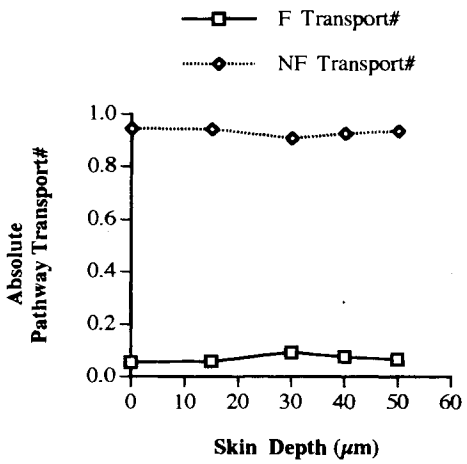

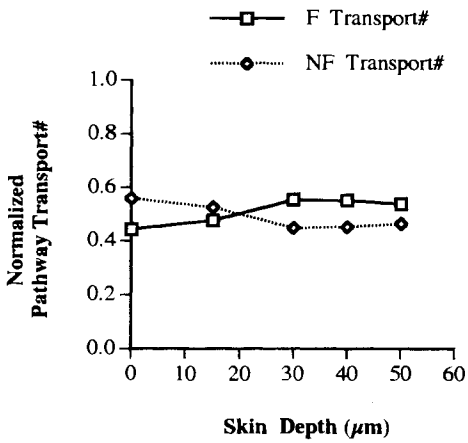

Fig. 6. Anodal iontophoresis of 7 KDa FITC-PLL for 16 hrs: absolute (above) and normalized (below) transport number values, as a function of skin depth via F and NF routes in HMS. Averaged data from three different skin sites (mean ± SD) in a single mouse are presented.

sible, nor that such an association would be without an effect on transport behavior.

It is important to pose the question again, therefore, as to which of the component driving forces contributes most importantly to the iontophoretic transport of polycationic PLLs. Electrorepulsion would seem to be the most obvious candidate, given the skin's permselectivity to positively-charged species, but the issue of potential skin tissue binding raises an important issue that may confound facile interpretation. It has been previously shown (24–27) that the iontophoretic delivery of cationic, lipophilic peptides can, in a concentration-dependent fashion, lead to the attenuation, and ultimately reversal, of electroosmotic solvent flow (in the normal anode-to-cathode direction) across the skin. It has been suggested that the positive charge of the peptide associates strongly with fixed negative sites in the membrane and that the adjacent lipophilic part of the molecule can then act as an "anchor" to induce a significant binding phenomenon. In this way, the net anionic charge of the membrane is progressively reduced, its permselectivity is lost and electroosmotic flow (anode-to-cathode) is shut down. Not surprisingly, perhaps, recent evidence from our laboratory (27) indicates that PLLs of MWs 2.7, 8.2 and 20 KDa show similar behavior, the effect increasing with increasing size of the polycation. The decrease in delivery observed, therefore, with increasing size of the FITC-labelled PLLs in these confocal experiments may be, at least in part, be due to the fact that (like the cationic, lipophilic peptides) the polycations are self-inhibiting their own transport by closing off the electroosmotic component. It has been demonstrated elsewhere (28) that this contribution becomes progressively more significant as the MW of the penetrant increases.

For all PLL experiments with iontophoresis, it was essential to establish that the fluorescent label remained associated with the polypeptide. Several aspects of the results confirm the integrity of the covalent linkage: (1) the delivery profiles were different for the PLLs of different MW—if the label had become unattached, there would probably have been no difference in the perceived transport as a function of MW; (2) in any case, had negatively-charged FITC label been hydrolyzed, it would have been attracted *away* from the skin towards the *driving* positive electrode; and (3) PLL-induced inhibition of anode-to-cathode electroosmosis would even further reduce the possibility of the FITC anion being delivered into the skin. Thus, it seems very likely that the fluorescent label does, in fact, remain covalently associated with the PLL polypeptide.

In conclusion, the results presented here demonstrate an inverse dependence of iontophoretic delivery upon the MW of the penetrant. While such a correlation has been previously deduced for negatively-charged species (29), this study is the first to consider cationic compounds and to attempt a quantitative evaluation of both extent of transport and mechanism of permeation (i.e., pathway of delivery). However, absolute conclusions cannot be drawn because of the confounding effects of larger cations on their mechanism of delivery (e.g., their ability to inhibit electroosmotic flow which, in some cases, represents the major means of transfer). Clearly, further work using carefully designed and selected probes is necessary to fully characterize this aspect of iontophoretic drug delivery across the skin.

ACKNOWLEDGMENTS

Financial support was provided by the U.S. National Institutes of Health (GM15585-03 and HD-27839) and The American Foundation for Pharmaceutical Education. Fluorescently-labeled compounds were generously provided by Novartis. We thank Martha Knight at Peptide Technologies Corporation for synthesis and molecular weight separation of FITC-labeled poly-L-lysines. We also thank Lauren Araiza and Yogeshvar Kalia for their practical and interpretive help.

REFERENCES

1. M. B. Delgado-Charro and R. H. Guy, (1997) in *Electronically-Controlled Drug Delivery*, eds. B. Berner & S. M. Dinh, (CRC Press, Boca Raton, FL), in press.
2. M. Clemessy, G. Couarraze, B. Bevan, and F. Puisieux. *Pharm. Res.* **12**:998–1002 (1995).
3. M. C. Heit, N. A. Monteiro-Riviere, F. L. Jayes, and J. E. Riviere. *Pharm. Res.* **11**:1000–3 (1994).
4. O. Siddiqui, Y. Sun, J. Liu, and Y. Chien. *J. Pharm. Sci.* **76**:341–345 (1987).
5. P. Lelawongs, J. C. Liu, and Y. W. Chien. *Int. J. Pharm.* **61**:179–188 (1990).
6. R. R. Burnette and D. Marrero. *J. Pharm. Sci.* **75**:738–743 (1986).
7. K. R. Oldenburg, K. T. Vo, G. A. Smith, and H. E. Selick. *J Pharm Sci.* **84**:915–21 (1995).
8. N. Yoshida and M. Roberts. *J. Control. Rel.* **25**:177–195 (1993).
9. S. Leduc. *Ann. D'Electrobiol.* **3**:545–560 (1900).
10. P. Wertz and D. Downing. *Science.* **217**:1261–1262 (1982).
11. N. G. Turner and R. H. Guy. *J. Invest. Derm.* submitted (1997).
12. P. Glikfeld, C. Cullander, R. S. Hinz, and R. H. Guy. *Pharm. Res.* **5**:443–446 (1988).
13. J. Keister and G. Kasting. *J. Control. Rel.* **4**:111–117 (1986).
14. H. Abramson and M. Engel. *Arch. Dermatol. Syphilol.* **44**:190–200 (1942).
15. H. Abramson and M. Gorin. *J. Phys. Chem.* **44**:1094–1102 (1940).
16. R. R. Burnette and B. Ongpipattanakul. *J. Pharm. Sci.* **76**:765–773 (1987).
17. S. Grimnes. *Acta. Derm. Ven. (Stockh).* **64**:93–98 (1984).
18. E. R. Scott, A. I. Laplaza, H. S. White, and J. B. Phipps. *Pharm. Res.* **10**:1699–1709 (1993).
19. C. Cullander and R. H. Guy. *Solid State Ionics.* **53–56**:197–206 (1992).
20. R. R. Burnette and B. Ongpipattanakul. *J. Pharm. Sci.* **77**:132–137 (1988).
21. C. Cullander and R. H. Guy. *J. Invest. Derm.* **97**:55–64 (1991).
22. G. T. McEwan, M. A. Jepson, B. H. Hirst, and N. L. Simmons. *Biochim. Biophys. Acta.* **1148**:51–60 (1993).
23. H. Takahashi, S. Matuoka, S. Kato, K. Ohki, and I. Hatta. *Biochim. Biophys. Acta.* **1110**:29–36 (1992).
24. M. B. Delgado-Charro and R. H. Guy. *Pharm Res.* **11**:929–35 (1994).
25. A. J. Hoogstraate, V. Srinivasan, S. M. Simms, and W. I. Higuchi. *J. Control. Rel.* **31**:41–47 (1994).
26. M. B. Delgado-Charro, A. M. Rodríguez-Bayón, and R. H. Guy. *J. Control. Rel.* **35**:35–40 (1995).
27. J. Hirvonen and R. H. Guy. *J. Control. Rel.* in press (1997).
28. M. Pikal. *Adv. Drug Del. Rev.* **9**:201–237 (1992).
29. P. G. Green, R. S. Hinz, A. Kim, F. C. Szoka, and R. H. Guy. *Pharm. Res.* **8**:1121–1127 (1991).